HHS Public Access

Author manuscript

Neuropharmacology. Author manuscript; available in PMC 2021 March 15.

Published in final edited form as:

Neuropharmacology. 2020 March 15; 165: 107831. doi:10.1016/j.neuropharm.2019.107831.

The kappa opioid receptor modulates GABA neuron excitability and synaptic transmission in midbrain projections from the insular cortex

Melanie M. Pina[1], **Dipanwita Pati**[1], **Lara S. Hwa**[1], **Sarah Y. Wu**[1], **Alexandra A. Mahoney**[1], **Chiazam G. Omenyi**[1], **Montserrat Navarro**[2], **Thomas L. Kash**[1,*]

[1]Bowles Center for Alcohol Studies, Department of Pharmacology, University of North Carolina at Chapel Hill, 104 Manning Drive, Chapel Hill, NC, 27599, USA

[2]Department of Psychology & Neuroscience, College of Arts and Sciences, University of North Carolina at Chapel Hill, Chapel Hill, North Carolina 27599, USA

Abstract

As an integrative hub, the insular cortex (IC) translates external cues into interoceptive states that generate complex physiological, affective, and behavioral responses. However, the precise circuit and signaling mechanisms in the IC that modulate these processes are unknown. Here, we describe a midbrain-projecting microcircuit in the medial aspect of the agranular IC that signals through the Gαi/o-coupled kappa opioid receptor (KOR) and its endogenous ligand dynorphin (Dyn). Within this microcircuit, Dyn is robustly expressed in layer 2/3, while KOR is localized to deep layer 5, which sends a long-range projection to the substantia nigra (SN). Using ex vivo electrophysiology, we evaluated the functional impact of KOR signaling in layer 5 of the IC. We found that bath application of dynorphin decreased GABA release and increased glutamate release on IC-SN neurons, but did not alter their excitability. Conversely, dynorphin decreased the excitability of GABA neurons without altering synaptic transmission. Pretreatment with the KOR antagonist nor-BNI blocked the effects of dynorphin on IC-SN neurons and GABA neurons, indicating that the changes in synaptic transmission and excitability were selectively mediated through KOR. Selective inhibition of IC GABA neurons using a KOR-derived DREADD recapitulated these effects. This work provides insight into IC microcircuitry and indicates that Dyn/KOR signaling may act to directly reduce activity of layer 5 GABA neurons. In turn, KOR-driven inhibition of GABA promotes disinhibition of IC-SN neurons, which can modulate downstream circuits. Our findings present a potential mechanism whereby chronic upregulation of IC Dyn/KOR signaling can lead to altered subcortical function and downstream activity.

(*)**Corresponding author :** Thomas L. Kash, PhD, John R. Andrews Distinguished Professor, Bowles Center for Alcohol Studies, Department of Pharmacology, University of North Carolina School of Medicine, Chapel Hill, NC 27599, USA, tkash@email.unc.edu.

Conflict of Interest: The authors declare no competing financial interests

1. Introduction

The insular cortex (IC) is a polytropic structure critical to a broad range of physiological and cognitive processes. The versatility of this structure is ostensibly due to the vast reciprocal connections that exist between it and an extensive network of cortical and subcortical structures [1]. Thus, the IC can be viewed as an anatomical hub that is responsible for interoceptive processing of multisensory information. It is not surprising then, that the IC has been found to play a role in a multitude of internals states.

For example, a dense literature has firmly established the role of the IC in the processing of pain [2, 3] and negative affective states like anxiety [4]. The IC has also been shown to mediate several processes integral to addiction such as craving and drug seeking [5–7]. Of note, the IC appears to be particularly involved in alcohol use disorder (AUD). Previous work has shown that alcohol dependence produces structural adaptions in the IC of both humans and rodents [8, 9]. In addition, the IC and its subcortical outputs are involved in modulating alcohol sensitivity and self-administration, as demonstrated in a series of elegant studies by Jaramillo and colleagues [10–13].

While the IC is partitioned cytoarchitecturally into three main divisions – granular, dysgranular, and agranular [14] – a majority of these studies have focused on the agranular division. Aptly named, the agranular IC has a unique cytoarchitectural organization with its lack of granular layer 4 and a merged layer 2/3 [15]. The IC expresses both the Gαi/o-coupled kappa opioid receptor (KOR) and its endogenous ligand dynorphin (Dyn) [16]. This is important in light of the growing evidence for Dyn/KOR modulation of mood disorders and the negative affective state that results in escalated drug consumption (reviewed in [17]).

Similar to the IC, the Dyn/KOR system is altered by chronic alcohol use and dependence. Specifically, chronic alcohol intake upregulates Dyn/KOR signaling, which may underlie the shift to an allostatic state that results in escalated consumption [18, 19]. This is supported by evidence that KOR antagonism suppresses alcohol self-administration in post-dependent rats, [20, 21] and alleviates withdrawal-induced anxiety-like behavior [22, 23]. Interestingly, KOR availability is reduced in the IC of human alcoholics, suggesting the IC may be an important site of Dyn/KOR plasticity in AUD [24].

In the present study, we evaluated the functional consequences of KOR activation on IC neuron excitability and synaptic transmission. We focused on layer 5 neurons, as KOR is predominately expressed postsynaptically in this layer of the rodent IC [25]. Here, we examined the effects of KOR activation on GABA neurons and a population of pyramidal neurons that project to the substantia nigra (SN). Like the IC, the SN is involved in both reward and aversion [26, 27], processes that are integral to addiction. Further, this area has been shown to be critical to withdrawal from abused drugs such as alcohol and sedative hypnotics [28]. Thus, we chose to focus on this long-range projection from the IC given the convergence of the IC, SN, and Dyn/KOR system in addiction and drug withdrawal.

Briefly, by using whole-cell patch clamp electrophysiology, we measured changes in excitability and synaptic transmission in layer 5 GABA and IC-SN neurons following acute bath application of dynorphin A. Based on our findings from these experiments, we then

tested the direct link between KOR-mediated inhibition of IC GABA neurons and changes in synaptic transmission on IC-SN neurons. Using a KOR-based DREADD (designer receptors exclusively activated by designer drugs; KORD) approach, we selectively inhibited GABA neurons and obtained whole-cell recordings from IC-SN neurons.

Finally, we used channelrhodopsin-assisted mapping to identify the neuronal populations in the SN that are modulated by IC inputs in order to determine the downstream impact of IC KOR signaling. In total, these studies yield novel insights into KOR signaling in the IC, as we show KOR activation directly reduced the excitability of layer 5 GABA neurons and increased the excitatory drive on IC pyramidal neurons that project onto both GABA and dopamine neurons of the SN.

2. Materials and methods

2.1. Mice

Adult male and female mice (>8 weeks old) were group-housed in a ventilated and temperature-controlled colony room that was kept on a 12:12-h light-dark cycle, with lights on at 7 a.m. Mice were provided access to rodent chow and water *ad libitum*. All strains of mice were bred in-house. Initially, preprodynorphin-IRES-Cre mice crossed to a R26-loxSTOPlox-L10-GFP reporter line (Dyn^{L10a}) [29, 30] were used to assess the expression of Dyn in the IC and the overlap of Dyn in SN-projecting IC neurons (Fig. 1). Following the discovery that Dyn neurons were confined to layer 2/3 of the IC and did not overlap with IC-SN neurons in layer 5, we utilized the L10-GFP negative mice for follow-up recordings in IC-SN neurons (n = 15). We selectively expressed KORD in IC GABA neurons, using a VGAT-IRES-Cre mouse line [31] (n = 4). To identify GABA neurons in the IC and SN, VGAT-IRES-Cre mice were crossed with the L10-GFP reporter line ($VGAT^{L10a}$, n = 16), as previously described [32]. Dopamine neurons in the SN were identified using a tyrosine hydroxylase-eGFP (TH^{eGFP}; n = 6) mouse strain [33, 34]. With the exception of optogenetic circuit mapping experiments, no more than 3 cells were obtained from each mouse per measure. All procedures were approved by the Institutional Animal Care and Use Committee of the University of North Carolina at Chapel Hill.

2.2. Surgical procedure

Mice were anesthetized with 4% isoflurane in O_2 and placed in a stereotaxic frame (Kopf Instruments). Sedation was maintained with 1–3% isoflurane for the duration of the procedure. Coordinates targeting the IC (from bregma in mm: AP +1.1, ML ±3.0, DV −3.8) and SN (AP: −3.40, ML: ±1.5, DV −4.1) were derived from a standard mouse brain atlas (Paxinos & Franklin, 2007). Microinjections were made using a 1 μl Neuros Syringe (Hamilton) with attached 33-gauge needle at a rate of 100 nL/min. For light-evoked synaptic transmission experiments, AAV5-CAMKIIα-hChR2(H134R)-mCherry (200 nL/side; ≥ 2.3×10^{13} vg/mL; Penn Vector Core) was injected into the IC of TH^{eGFP} and $vGAT^{L10a}$ mice. In chemogenetic experiments, AAV8-hSyn-dF-HA-KORD-IRES-mCitrine (300 nL/side; 2.1×10^{13}; Addgene) was injected unilaterally into the IC of vGAT-Cre mice. To retrogradely label SN-projecting IC cells, mice received bilateral infusions (200 nL/side) of retrograding fluorescent microspheres (Red RetroBeads™ IX, Lumafluor Inc.), a retrograde AAV

carrying a cre-dependent fluorescent protein (AAVrg-CAG-tdTomato; 4×10^{12} vg/mL; Addgene), or a fluorescent retrograde dye (Fluoro-Gold, 4% in 0.9% saline; Fluorochrome) into the SN. Following injections, the needle was left in place for 5 minutes to allow for diffusion. To minimize postoperative discomfort, mice were given access to acetaminophen in their drinking water (0.4 mg/mL) for 7 days following surgery.

2.3. Immunohistochemistry

Mice were deeply anesthetized with Avertin (250 mg/kg, IP) and transcardially perfused with chilled 0.01 M phosphate buffered saline (PBS, pH 7.4) followed by 4% paraformaldehyde (PFA). Brains were removed and immersed in 4% PFA overnight, then stored in 30% sucrose/PBS before 45-μm coronal sections were taken on a vibratome (Leica VT1000 S). Free-floating sections were stored at −20°C in 50% glycerol in PBS until being processed for double immunofluorescence (IF). Slices containing the Dyn-enriched region (Fig. 1) of the IC (+1.54 to +0.38 mm anterior to bregma) and the SN (−2.7 to −4.0 mm posterior to bregma) were washed in PBS, then blocked and permeabilized in 5% normal donkey serum or normal goat serum/0.3% Triton X-100/PBS for 45 min. Tissue was then incubated overnight with gentle agitation at 4°C in a blocking solution with primary antibodies: chicken polyclonal anti-GFP (1:2000, Aves Labs), rabbit polyclonal anti-RFP (1:2000, Abcam), guinea pig anti-Fluoro-Gold (1:3000, Protos Biotech). Sections were then rinsed, blocked for 45 min, and incubated at room temperature for 2 h in blocking solution containing fluorophore-conjugated secondary antibodies: Alexa Fluor 488 donkey anti-chicken or goat anti-chicken IgG, Cy3 donkey anti-rabbit or goat anti-guinea pig IgG, (1:400 each, Jackson ImmunoResearch). All sections were rinsed in PBS after the final incubation, mounted with Vectashield Hardset Mounting Medium with DAPI (Vector Labs), and imaged on a Zeiss LSM 800 confocal microscope or an Olympus BX43 with attached optiMOS sCMOS camera (QImaging). For presentation, channels were merged and images cropped and contrast adjusted in Zen Lite (Zeiss) or ImageJ (NIH).

2.4. Slice electrophysiology

For whole-cell patch-clamp electrophysiological recordings, mice were rapidly decapitated under isoflurane anesthesia, and their were brains quickly extracted and immersed in ice-cold sucrose artificial cerebrospinal fluid (aCSF), containing (in mM) 194 sucrose, 20 NaCl, 4.4 KCl, 2 CaCl2, 1 MgCl2, 1.2 NaH2PO4, 10 D-glucose and 26 NaHCO3 saturated with 95% O2 / 5% CO2. Coronal slices from the IC (300 μM) and SN (250 μM) were prepared on a Leica VT 1200s vibratome (Leica Biosystems) and then transferred to a heated oxygenated holding chamber containing normal aCSF (in mM: 124 NaCl, 4.4 KCl, 1 NaH2PO4, 1.2 MgSO4, 10 D-glucose, 2 CaCl2, and 26 NaHCO3). Slices were allowed to equilibrate for at least 30 minutes before being transferred to a submerged recording chamber superfused at a rate of 2 mL/min with oxygenated aCSF that was maintained at approximately 30°C. Neurons were visualized under a 40x immersion objective using video-enhanced differential interference contrast (Olympus). Fluorescent cells and ChR2-expressing fibers were visualized using a mercury arc lamp-based system. Whole-cell patch clamp recordings were made using recording electrodes (2–4 MΩ) pulled from thin-walled borosilicate glass capillaries with a Flaming-Brown Micropipette Puller (Sutter P-97, Sutter Instruments). Signals were acquired using an Axon Multiclamp 700B amplifier (Molecular Devices),

digitized at 10 kHz, filtered at 3 kHz, and analyzed in pClamp 10.7 (Molecular Devices). Access resistance (Ra) was monitored throughout experiments and cells with changes in Ra greater than 20% of the initial value were discarded.

Excitability experiments were performed in current clamp mode using a potassium gluconate-based intracellular solution (K-Gluc; in mM: 135 K-gluconate, 5 NaCl, 2 MgCl2, 10 HEPES, 0.6 EGTA, 4 Na2ATP, 0.4 Na2GTP, pH 7.3, 289–292mOsm). Cells were allowed to stabilize for 2–5 min, and current was then injected to hold cells at a common membrane potential of −70 mV. Changes in the current-injected firing of action potentials were evaluated by measuring rheobase (minimum current required to elicit an action potential) and the number of action potentials fired at increasing 50 pA current steps (0 to 650 pA).

Spontaneous synaptic activity was assessed in voltage clamp mode using a cesium methanesulfonate-based intracellular solution (Cs-Meth; in mM: 135 cesium methanesulfonate, 10 KCl, 1 MgCl2, 0.2 EGTA, 4 MgATP, 0.3 Na2GTP, 20 phosphocreatine, pH 7.3, 285–290 mOsm with 1mg/mL QX-314). Cells were clamped at a holding potential of −55 mV to record spontaneous excitatory postsynaptic currents (sEPSCs) and +10 mV to record spontaneous inhibitory postsynaptic currents (sIPSCs) within the same neuron, as previously described [35, 36]. Baseline recordings were obtained at −55 mV and +10 mV, before drugs were bath applied at +10 mV for 10 min. Recordings were obtained continuously at +10 mV during drug application, given our previous finding that Dyn directly inhibited local GABA neurons. Immediately following, cells were again clamped at −55 mV and a final recording of sEPSC was obtained in the presence of drug. Event frequency and amplitude were analyzed in pClamp 11 (Molecular Devices) over a period of 120 s or the first 500 events at baseline and during the final 120 s of drug application at +10 mV and −55 mV. To pharmacologically isolate miniature IPSCs, tetrodotoxin (TTX; 500 nM) and kynurenic acid (3 mM) were added to the bath solution. Recording electrodes were filled with (in mM) 70 KCl, 65 K–gluconate, 5 NaCl, 10 HEPES, 0.6 EGTA, 4 Na-ATP, 0.4 Na-GTP, pH 7.25, 290–295 mOsm w/ 1 mg/mL QX-314 and cells were voltage clamped at −70 mV. Data from mIPSC recordings were analyzed similarly to sPSCs, wherein the event frequency and amplitude were measured over a period of 120 s or the first 500 events at baseline and during the final 120 s of drug application.

For optogenetic experiments, brains were first evaluated for optically evoked action potentials in the injection region of the IC using a K-Gluc intracellular recording solution. Stimulation parameters included ten 5 ms blue light (490 nm) pulses at 1, 2, 5, 10, 15, and 20 Hz. Light-evoked synaptic transmission recordings in the SN were conducted in voltage clamp mode using a Cs-Meth intracellular solution to detect optically-evoked EPSCs (−55 mV) and IPSCs (+10 mV) within each neuron. Fibers expressing ChR2 in the SN were stimulated using two 5 ms blue light pulses with an interstimulus interval of 50 ms.

2.5. Pharmacology

The endogenous kappa-opioid receptor agonist, dynorphin A-(1–17) (Tocris) was bath applied for 10 min at a concentration of 300 nM as previously reported [29]. Endopeptidase inhibitors bestatin HCl (10 μM, Sigma-Aldrich) and DL-Thiorphan (1 μM, Sigma-Aldrich)

were combined with dynorphin A [37]. A previous study has shown that KOR agonism is not reversed by the KOR antagonist Nor-Binaltorphimine dihydrochloride (nor-BNI) [29]. Thus, nor-BNI (100 nM, Tocris) was added to the extracellular aCSF solution and pre-applied to slices for at least 15 min prior to experiments. For chemogenetic experiments, salvinorin B (SalB; Tocris) was bath applied for 10 min at a 100 nM concentration [38].

2.6. Experimental Design and Statistical Analysis

To assess for sex differences, data were first analyzed by two-way (drug × sex) or three-way (drug × current × sex) mixed model ANOVA. Two-way (drug × sex) mixed model ANOVA was used to examine the effect of drug on rheobase, sEPSC/sIPSC/mIPSC frequency and amplitude, and E/I ratio. Dynorphin A effects on spiking frequency as a function of current were assessed via three-way mixed model ANOVA (drug × current × sex). Where analyses yielded no significant interactions by sex or main effect of sex, data were collapsed across both sexes and analyzed by paired t-test or two-way mixed model ANOVA (drug × current). Significance threshold was set at $\alpha = 0.05$. For all measures, mean ± SEM by sex are provided in Supplementary Table 1. All data were analyzed using JASP 0.9 (JASP Team).

3. Results

3.1. Kappa opioid receptor modulation of SN-projecting IC neurons

As previously reported [39, 40], the IC sends a long-range projection to the SN (Fig. 1). We initially identified this projection using viral-mediated anterograde tracing from pyramidal neurons in the IC. Briefly, injections of AAV5-CAMKIIα-ChR2-mCherry (200 nL/side) were made into the IC, which resulted in robust labeling of IC fibers in the SN (Fig. 1A). Next, this projection was confirmed by injecting the retrograde tracer Fluoro-Gold (200 nL/side) into the SN. Retrograde tracing revealed that IC inputs to the SN are localized to deep layer 5 and 6 and do not appear to robustly overlap with Dyn cells in this region, which are largely confined to layer 2/3 (Fig. 1B–C).

Given that a previous study has shown that KOR is expressed postsynaptically in layers 5 and 6 of the IC [25], we evaluated the effect of KOR activation on IC-SN neurons to determine whether this cell population could be modulated by locally acting Dyn. To isolate IC-SN neurons for whole-cell patch clamp electrophysiology, fluorescent retrobeads (200 nL/side) were bilaterally injected into the SN, and labeled neurons in the IC were recorded from 7–10d thereafter. The effect of KOR activation on IC-SN neuron excitability was first assessed by measuring current-injected firing at baseline and after 10 min bath application of 300 nM dynorphin A (Fig. 2). Neurons were held at −70 mV in current clamp mode to account for variability in resting membrane potential, and dynorphin A-induced changes in rheobase (the minimum current required to elicit an action potential) and the number of action potentials fired across a series of increasing current steps were assessed. In IC-SN neurons, we found that dynorphin A did not shift the rheobase from baseline ([$t(13) = 1.00$, $p = 0.334$]; Fig. 2D) or impact the number of action potentials fired at increasing current steps (Fig. 2E), as there was a main effect of current [$F(12,156) = 69.16$, $p < 0.001$] but not drug [$F(1,13) = 2.73$, $p = 0.123$] and no drug × current interaction [$F(12,156) = 1.18$, $p = 0.304$].

Next, the impact of KOR activation on spontaneous synaptic transmission in IC-SN neurons was examined (Fig. 3). Dynorphin A-induced changes in the ratio of excitatory/inhibitory (E/I) transmission were evaluated in individual IC-SN neurons. This was accomplished by holding cells in voltage clamp mode at −55 mV and +10 mV, respectively, to measure both spontaneous excitatory postsynaptic current (sEPSC) and spontaneous inhibitory postsynaptic current (sIPSC). In contrast to its lack of effect on excitability, dynorphin A significantly increased sEPSC frequency [$t(11) = 2.67$, $p = 0.022$] in IC-SN neurons (Fig. 3B). Additionally, sIPSC frequency was significantly reduced by dynorphin A as revealed by a main effect of drug [$F(1,10) = 11.40$, $p = 0.007$] but no drug × sex interaction [$F < 1$]. Interestingly, we found a main effect of sex [$F(1,10) = 7.89$, $p = 0.018$], as sIPSC frequency was significantly higher in female compared to male mice. No effect on sEPSC amplitude [$t(11) = 2.03$, $p = 0.068$] or sIPSC amplitude [$t(11) = 1.51$, $p = 0.160$] was found. Dynorphin A wash-on significantly increased sEPSC/sIPSC (E/I) ratio in IC-SN cells in a sex-dependent fashion (Fig. 3D), as indicated by significant main effects of drug [$F(1,10) = 12.77$, $p = 0.005$] and sex [$F(1,10) = 22.31$, $p < 0.001$] and an interaction of drug × sex ([$F(1,10) = 11.58$, $p = 0.007$]. Post-hoc analyses revealed that dynorphin A increased E/I ratio in males [$t(5) = 3.49$, $p = 0.017$] but not females [$t(5) = 1.71$, $p = 0.147$]. To confirm that these dynorphin A-induced effects on IC-SN neurons were mediated through KOR, the KOR antagonist nor-BNI (100 nM) was included in the aCSF bath solution, and slices were pretreated for at least 15 min prior to recording. In the presence of nor-BNI, dynorphin A did not alter spontaneous synaptic transmission from baseline in IC-SN neurons (Fig. 3F–I), as no significant differences were found in sEPSC frequency [$t(9) = 1.08$, $p = 0.308$], sEPSC amplitude [$t(9) = 0.71$, $p = 0.495$], sIPSC frequency [$t(9) = 1.22$, $p = 0.252$], or sIPSC amplitude [$t(9) = 1.78$, $p = 0.110$] following dynorphin A wash-on, and there was no shift in the E/I ratio [$t(9) = 0.55$, $p = 0.595$]. Lastly, we tested whether KOR activation reduced sIPSC frequency through inhibiting activity-dependent GABA release on IC-SN neurons (Fig. 4). Action potential-independent miniature inhibitory postsynaptic current (mIPSC) was isolated by bath application of TTX (500 nM) and kynurenic acid (3 mM). Following dynorphin A application, mIPSC frequency [$t(9) = 0.23$, p 0.822] and amplitude [$t(9) = 0.44$, $p = 0.668$] were not significantly reduced compared to baseline (Fig 4B–C), indicating that the effect of KOR activation on inhibitory neurotransmission in IC-SN cells is network-activity dependent. Collectively, these results indicate that KOR activation does not modulate the excitability of IC-SN neurons through a postsynaptic mechanism, but does act presynaptically to increase release of glutamate and decrease action potential-dependent release of GABA onto these cells. In males, the net effect of this phenomenon is a significant shift in the E/I ratio, which results in a state of increased excitatory synaptic drive in IC-SN neurons.

3.2. Kappa opioid receptor modulation of GABA neurons in layer 5 of the IC

Given that KOR activation decreased GABA release onto IC-SN neurons, we next evaluated whether KOR could modulate the activity of local GABA neurons contained in layer 5 of the IC. GABA neurons were identified in $vGAT^{L10a}$ mice and whole-cell recordings were obtained at baseline and following 10 min bath application of dynorphin A (300 nM). To evaluate KOR activation on vGAT neuron excitability, cells were held at −70 mV in current clamp mode and dynorphin A-induced changes in rheobase and the number of action

potentials fired across increasing current steps were assessed (Fig. 5). In vGAT neurons held at a common membrane potential of −70 mV, dynorphin A significantly increased the rheobase ([t(9) = 2.63, p = 0.027]; Fig. 5B) and reduced the number of action potentials fired across current steps (Fig. 5D). This was supported by significant main effects of drug [F(1,9) = 6.08, p = 0.036] and current [F(9,81) = 12.38, p < 0.001], but no drug × current interaction [F(9,81) = 1.18, p = 0.318]. To determine whether dynorphin A-induced changes in vGAT neuron excitability were mediated through KOR, slices were pretreated with nor-BNI, as previously described. In the presence of nor-BNI, dynorphin A did not increase rheobase compared to baseline ([t(7) = 1.25, p = 0.250], Fig. 5C) and did not decrease spiking frequency across current steps (Fig. 5E), as indicated by a main effect of current [F(9,63) = 5.72, p < 0.001] but not drug [F(1,7) = 0.18, p = 0.687], and no drug × current interaction [F(9,63) = 0.50, p = 0.870]. These findings indicate that dynorphin A reduced the excitability of GABA neurons in layer 5 of the IC through a KOR-dependent postsynaptic mechanism.

We next assessed the impact of KOR activation on excitatory/inhibitory (E/I) drive in vGAT neurons (Fig. 6). As described, both sEPSC and sIPSC were measured by voltage clamping the membrane potential of individual neurons at −55 mV and +10 mV, respectively. Following dynorphin A application in layer 5 vGAT neurons, there was no change from baseline in sEPSC frequency [t(11) = 1.86, p = 0.089] or amplitude [t(11) = 0.39, p = 0.704] (Fig. 6B–C). In addition, sIPSC frequency was not significantly altered by dynorphin A (Fig. 6F), as there was no main effect of drug [F(1,10) = 4.57, p = 0.058] and no drug × sex interaction [F(1,10) = 1.51, p = 0.247]. Here, we found a significant main effect of sex on sIPSC frequency [F(1,10) = 34.94, p = 0.031], as females had a lower overall mean sIPSC frequency compared to males. There was no effect of dynorphin A on sIPSC amplitude (t[11] = 0.80, p = 0.440]; Fig. 6G). As expected, given its lack of effect on sPSCs, we found that dynorphin A did not significantly alter E/I ratio ([t(11) = 1.77, p = 0.105], Fig. 6H). These findings suggest that KOR activation does not alter presynaptic release of GABA or glutamate onto layer 5 GABA neurons of the IC. Taken together, our results suggest that KOR modulates the activity of layer 5 IC GABA neurons through a postsynaptic mechanism, whereby KOR activation directly reduces neuronal excitability but does not alter excitatory or inhibitory neurotransmission onto these neurons.

3.3. Chemogenetic inhibition of IC GABA neurons alters E/I ratio in IC-SN neurons

To directly test the effect of IC GABA inhibition on synaptic transmission in IC-SN neurons, we used a chemogenetic approach in which we unilaterally injected an AAV carrying a cre-dependent KORD construct (AAV8-hSyn-dF-HA-KORD-IRES-mCitrine) into the IC of vGAT-cre mice. This KOR-based DREADD is selectively activated by the otherwise inert ligand salvinorin B (SalB), and is capable of producing robust neuronal silencing [38]. The contralateral hemisphere of the IC served as a non-KORD expressing control. For long-term labeling of IC-SN neurons in these mice, a retrograde AAV-tdTomato (AAVrg-CAG-tdTomato) was injected bilaterally into the SN.

We first confirmed the functional expression of KORD by obtaining current clamp recordings from mCitrine-expressing neurons in the IC and bath applying SalB (100 nM).

As previously reported at this concentration [38], we found that SalB hyperpolarized KORD-expressing neurons in the IC (Fig. 7B). In KORD-expressing tissue, bath application of SalB increased sEPSC frequency in IC-SN neurons as indicated by a significant main effect of drug [$F(1,6) = 13.55$, $p < 0.01$] (Fig. 7C). While we found no interaction of drug × sex [$F(1,6) = 4.25$, $p = 0.090$], analyses revealed a main effect of sex [$F(1,6) = 7.09$, $p = 0.037$] as female mice exhibited a lower overall frequency of sEPSCs compared to males. Following SalB wash-on, sIPSC frequency in IC-SN neurons was significantly reduced [$t(7) = 4.12$, $p = 0.004$] (Fig. 7D). We found no effect of SalB on sEPSC amplitude ($p = 0.110$) or sIPSC amplitude ($p = 0.594$). As expected, given the effects of KORD activation on sPSC frequency, we found that SalB significantly increased E/I ratio [$t(7) = 2.95$, $p = 0.021$] (Fig. 7E). In control tissue (Fig. 7G–J), SalB did not alter sEPSC frequency or amplitude (p's > 0.4), sIPSC frequency or amplitude (p's > 0.4), or E/I ratio ($p = 0.656$). These findings show that SalB-mediated activation of KORD in IC GABA neurons results in increased glutamate release, decreased GABA release, and increased excitatory drive onto IC-SN neurons. Notably, this recapitulates our previous findings, which showed increased excitatory drive in IC-SN neurons following dynorphin A wash-on and suggests that these effects are a direct result of KOR-induced inhibition of GABA neurons in the IC.

3.4. Modulation of SN GABA and dopamine by layer 5 IC inputs

Given our finding that KOR activation increased the E/I ratio in IC-SN neurons of male mice, we sought to determine the downstream cell populations in the SN that may be impacted by shifts in synaptic transmission onto IC neurons. In the SN, neurons can be broadly classified into two major populations, GABA and dopamine, which are compartmentalized in the pars reticulata (SNpr) and pars compacta (SNpc), respectively [41, 42]. Thus, we used the transgenic reporter strains $vGAT^{L10a}$ (n = 3) to target GABA neurons and TH^{eGFP} (n = 6) to target dopamine neurons within the SN. As illustrated in Fig. 8A, all mice received bilateral IC injections of an AAV encoding for channelrhodopsin-2 under the control of calcium/calmodulin-dependent protein kinase II alpha (AAV5-CAMKIIα-ChR2-mCherry) promoter, to restrict expression of ChR2 to pyramidal neurons of the IC [43, 44]. Recordings were obtained from ChR2-expressing neurons in the injection region of the IC to confirm optically-evoked action potentials in these neurons (Fig. 8B–C). To determine the cell populations innervated by layer 5 IC neurons, optically evoked excitatory (oEPSCs) and inhibitory postsynaptic currents (oIPSCs) were recorded in SN vGAT and TH neurons using a paired 5 ms 490 nm light-pulse. As shown in Fig. 8D–F, we observed time-locked monosynaptic oEPSCs in 33.3% of SN vGAT neurons (n = 4 of 12), which had an average onset time (latency) after light stimulation of 1.65 ± 0.42 ms and mean peak amplitude of 116 ± 42 pA. Polysynaptic oIPSCs with a slower onset latency of 3.08 ± 0.21 ms ([$t(5) = 2.72$, $p = 0.040$], compared to oEPSC) and a mean peak amplitude of 387 ± 92 pA were observed in 25% of SN vGAT neurons (n = 3 of 12; Fig. 8E–F). Of the total neurons that exhibited an oEPSC, 75% (n = 3 of 4) also displayed an oIPSC. Conversely, oIPSCs were only observed in cells that exhibited an oEPSC. In neurons with both oEPSCs and oIPSCs, we found that the ratio of oEPSC/oIPSC peak amplitudes was 0.61 ± 0.06, thus suggesting that the functional result of glutamatergic input from the IC to SN vGAT neurons may be increased inhibitory tone. In SN TH neurons (Fig. 8G–I), 42.8% (n = 12 of 28) showed monosynaptic oEPSCs with a rapid onset latency of 0.58 ± 0.18 ms and average peak

amplitude of 184 ± 48 pA. However, oIPSCs were more prevalent in dopamine neurons as compared to GABA neurons of the SN, as 46.4% of TH neurons (n = 13 of 28) showed polysynaptic oIPSCs that had more delayed latencies, averaging 3.06 ± 0.16 ms ([t(23) = 10.32, p < 0.001], compared to oEPSC) and mean peak amplitude of 249 ± 67 pA. In SN TH neurons with an oEPSC, 91.7% (n = 11 of 12) also exhibited an oIPSC and in neurons with an oIPSC, 84.6% (n = 11 of 13) exhibited an oEPSC. Further, of the total oIPSCs, only 2 of 13 were observed in the absence of an oEPSC and both had latencies of greater than 3.6 ms and amplitudes < 20 pA. In contrast to the potential inhibitory impact of IC input to SN vGAT neurons, our data suggest that IC input to SN TH neurons may result in increased excitation, as the ratio of oEPSC/oIPSC amplitudes in these neurons was 1.21 ± 0.41. Overall, these data indicate that the IC makes a functional connection with the SN, releasing glutamate onto a subpopulation of GABA and dopamine neurons of the SN.

4. Discussion

In the present experiments, we show that KOR modulates two distinct neuronal populations in layer 5 of the IC. Using ex vivo electrophysiology, we found that bath application of dynorphin A altered spontaneous synaptic transmission in IC-SN neurons and increased their excitatory drive but did not impact their excitability. Conversely, dynorphin A decreased the excitability of layer 5 IC GABA neurons without altering synaptic transmission. Pretreatment with the KOR antagonist nor-BNI blocked the effects of dynorphin A on IC-SN neurons and GABA neurons, indicating that the changes in synaptic transmission and excitability were selectively mediated through KOR. We then recapitulated the effects of dynorphin A on E/I in IC-SN neurons by directly inhibiting IC GABA neurons using a KOR-based DREADD approach.

4.1. KOR modulation of an IC microcircuit

The agranular cortex contains a distinct intrinsic microcircuit, wherein layer 2/3 cells project interlaminarly into layer 5 [45], which serves as the major cortical output layer. In our initial anatomical tracing work, we identified a discrete population of Dyn-containing neurons clustered in layer 2/3 of the IC. Adjacent to these Dyn neurons in the IC, we identified a population of pyramidal neurons in layer 5 that project to the SN. Using a viral approach, we confirmed this long-range IC projection to the SN is functional and serves to innervate both GABA and dopamine neurons in the SNpr and SNpc, respectively. Given the proposed microcircuitry of the agranular cortex, it is possible that layer 2/3 Dyn neurons modulate layer 5 neurons of the IC where KOR is expressed postsynaptically [25]. This may constitute a unique laminar microcircuit in the IC that signals locally through Dyn/KOR to modulate midbrain dopamine activity. Thus, we sought to directly test the functional consequences of KOR activation on layer 5 neurons in the IC using the endogenous KOR agonist dynorphin A.

When bath applied, we found that dynorphin A did not impact the excitability of IC-SN neurons. However, dynorphin A had a robust effect on spontaneous synaptic transmission in IC-SN neurons such that it resulted in an increase in sEPSC frequency and a concurrent decrease in sIPSC frequency. These results indicate that KOR does not directly modulate the

excitability of IC-SN neurons through a postsynaptic mechanism, but does act presynaptically to increase release of glutamate and decrease release of GABA onto these cells, shifting their E/I ratio to favor a state of increased excitatory drive. Interestingly, we found that in layer 5 GABA neurons, dynorphin A produced a decrease in excitability, indicating that KOR is expressed postsynaptically on layer 5 IC GABA neurons. This suggests a possible mechanism by which KOR activation reduces GABA release onto local IC-SN neurons, through direct inhibition of proximal GABAergic interneurons, which are known to gate cortical signaling and shape the dynamics of cortical networks [46]. In support of this, when we blocked action-potential mediated firing with TTX, we found no reduction in mIPSC frequency, suggesting that KOR activation reduces activity-dependent release of GABA on IC-SN neurons. Cortical interneurons have been shown to tightly regulate the activity of layer 5 pyramidal neurons and control output from the cortex through both perisomatic and dendritic inhibition [47]. It is possible that the direct inhibition of GABAergic transmission in the IC disinhibited pyramidal neurons, thereby contributing to the increase in glutamate release we observed on IC-SN neurons following dynorphin A. Hence, our findings indicate that KOR activation reduces inhibitory input and therefore potentially disinhibits IC-SN neurons in order to modulate downstream circuits. Altogether, our results reveal novel insight into the functional role KOR plays within the IC and its modulation of synaptic inputs onto IC-SN neurons.

4.2. Modulation of SN dopamine and GABA by IC inputs

Consistent with other reports, we found a long-range input to the SN from the IC [1, 39]. Using ChR2-assisted circuit mapping and retrograde tracing, we discovered this input is functional and arises from a subpopulation of pyramidal neurons in layer 5 of the IC. Within the SN, we found that IC projection neurons innervated the two major neuronal populations of this region, dopamine and GABA. As previously reported, we observed a direct input from the IC to dopamine neurons in the SNpc [40], a subdivision of the SN containing the A9 cell group [48]. Here, optical stimulation of ChR2-expressing IC neuron terminals resulted in a time-locked release of glutamate on nearly half of the dopamine neurons that we recorded. We also found polysynaptic release of GABA in the same SNpc dopamine neurons. As a principle source of GABAergic input to SNpc dopamine neurons is known to arise from axon collaterals of SNpr GABA projection neurons [49, 50], this likely reflects the concomitant innervation of SNpr GABA neurons by IC inputs. Accordingly, we found that optical stimulation also resulted in time-locked glutamate release on SNpr GABA neurons and delayed polysynaptic GABA current. Considering that KOR activation increased excitatory drive on IC-SN neurons, it is likely that the disinhibition of IC-SN neurons leads to increased glutamate release on to both dopamine and GABA neurons in the SN. However, it is unclear what the net result of this increased IC input would be, given that both dopamine and GABA neurons received direct IC innervation and delayed inhibition. Based on the ratio of E/I peak amplitudes in SN vGAT and TH neurons, it is possible that increased IC input to the SN inhibits the activity of GABA neurons and enhances dopamine neuron activity. Thus, future studies should aim to determine the behavioral effect of increased IC input into the SN as well as the physiological impact in sites downstream of SN.

4.3. Sex differences in basal IC activity and KOR signaling

Previous studies have shown sex differences in both the expression and function of KOR in the human and rodent IC [51, 52]. In the present experiments, we assessed sex differences in response to KOR activation within the IC by using male and female mice. Whereas dynorphin A reduced the excitability of vGAT neurons in both male and female mice, it increased the E/I ratio in IC-SN neurons of male mice alone.

Despite an interaction between KOR activation and sex in IC-SN neurons, the effects of dynorphin A on vGAT neurons did not differ between male and female mice. The interaction of sex and dynorphin A treatment on E/I ratio in IC-SN neurons may reflect some of the main effects of sex that we found in basal function in both IC-SN neurons and IC vGAT neurons. For instance, sIPSC frequency in IC-SN neurons was higher in female mice at baseline and following dynorphin A wash-on. This resulted in a lower overall E/I ratio in IC-SN neurons in females than in males. Moreover, female mice exhibited a lower frequency of sIPSC in IC vGAT neurons compared to male mice, indicating that they have a reduced inhibitory tone on this cell population. Notably, reduced GABA release on vGAT neurons in the female IC may contribute to the higher sIPSC frequency and dampened excitatory drive we observed in IC-SN neurons, as lack of inhibition of vGAT cells would be expected to promote a greater overall inhibitory tone in this region.

These findings are interesting and suggest a possible mechanism for further investigation, especially given the higher incidence of anxiety and depression in women [53] and the insula's role in these affective states [4, 54]. Moreover, it is possible that greater engagement of the Dyn/KOR system (e.g., after chronic exposure to drugs of abuse and stress) may be necessary to unmask additional sex-dependent differences in KOR signaling, thus highlighting an important area of future work.

5. Conclusions

These experiments describe a unique cortical microcircuit that signals through KOR. Collectively, our results demonstrate that in the IC, KOR functions to directly modulate the activity of layer 5 GABA neurons, which locally regulate a midbrain-projecting population of pyramidal neurons. These projection neurons, found in layer 5 of the IC, innervate both dopamine and GABA neurons in the SN. Overall, this suggests a potential mechanism whereby chronic upregulation of Dyn/KOR signaling in the IC can lead to altered subcortical function and activity in downstream pathways. Future work is needed to determine the behavioral consequences of KOR activation in the IC and the mechanisms by which Dyn/KOR signaling may be upregulated in this region.

Supplementary Material

Refer to Web version on PubMed Central for supplementary material.

Acknowledgements

This work was supported by the National Institutes of Health [grant numbers F32AA026485 (MMP), R01AA019454 (TLK), U01AA020911 (TLK), R01AA025582 (TLK), R01AA025582-S1 (TLK/MMP), and P60AA011605 (TLK/MN)]

6. References

1. Saper CB, Convergence of autonomic and limbic connections in the insular cortex of the rat. J Comp Neurol, 1982 210(2): p. 163–73. [PubMed: 7130477]
2. Starr CJ, et al., Roles of the insular cortex in the modulation of pain: insights from brain lesions. J Neurosci, 2009 29(9): p. 2684–94. [PubMed: 19261863]
3. Lu C, et al., Insular Cortex is Critical for the Perception, Modulation, and Chronification of Pain. Neurosci Bull, 2016 32(2): p. 191–201. [PubMed: 26898298]
4. Paulus MP and Stein MB, An insular view of anxiety. Biol Psychiatry, 2006 60(4): p. 383–7. [PubMed: 16780813]
5. Contreras M, Ceric F, and Torrealba F, Inactivation of the interoceptive insula disrupts drug craving and malaise induced by lithium. Science, 2007 318(5850): p. 655–8. [PubMed: 17962567]
6. Moschak TM, Wang X, and Carelli RM, A Neuronal Ensemble in the Rostral Agranular Insula Tracks Cocaine-Induced Devaluation of Natural Reward and Predicts Cocaine Seeking. J Neurosci, 2018 38(39): p. 8463–8472. [PubMed: 30126972]
7. Naqvi NH and Bechara A, The hidden island of addiction: the insula. Trends Neurosci, 2009 32(1): p. 56–67. [PubMed: 18986715]
8. Chattopadhyay S, et al., Structural Changes in the Insular Cortex in Alcohol Dependence: A cross sectional study. Iran J Psychiatry, 2011 6(4): p. 133–7. [PubMed: 22952538]
9. Chen H, He D, and Lasek AW, Repeated Binge Drinking Increases Perineuronal Nets in the Insular Cortex. Alcohol Clin Exp Res, 2015 39(10): p. 1930–8. [PubMed: 26332441]
10. Jaramillo AA, et al., Functional role for suppression of the insular-striatal circuit in modulating interoceptive effects of alcohol. Addict Biol, 2017.
11. Jaramillo AA, et al., Modulation of sensitivity to alcohol by cortical and thalamic brain regions. Eur J Neurosci, 2016 44(8): p. 2569–2580. [PubMed: 27543844]
12. Jaramillo AA, et al., Functional role for cortical-striatal circuitry in modulating alcohol self-administration. Neuropharmacology, 2018 130: p. 42–53. [PubMed: 29183687]
13. Jaramillo AA, et al., Silencing the insular-striatal circuit decreases alcohol self-administration and increases sensitivity to alcohol. Behav Brain Res, 2018 348: p. 74–81. [PubMed: 29660441]
14. Gogolla N, The insular cortex. Curr Biol, 2017 27(12): p. R580–R586. [PubMed: 28633023]
15. Van De Werd HJ and Uylings HB, The rat orbital and agranular insular prefrontal cortical areas: a cytoarchitectonic and chemoarchitectonic study. Brain Struct Funct, 2008 212(5): p. 387–401. [PubMed: 18183420]
16. Chavkin C, James IF, and Goldstein A, Dynorphin is a specific endogenous ligand of the kappa opioid receptor. Science, 1982 215(4531): p. 413–5. [PubMed: 6120570]
17. Wee S and Koob GF, The role of the dynorphin-kappa opioid system in the reinforcing effects of drugs of abuse. Psychopharmacology (Berl), 2010 210(2): p. 121–35. [PubMed: 20352414]
18. Koob GF, Addiction is a Reward Deficit and Stress Surfeit Disorder. Front Psychiatry, 2013 4: p. 72. [PubMed: 23914176]
19. Sirohi S, Bakalkin G, and Walker BM, Alcohol-induced plasticity in the dynorphin/kappa-opioid receptor system. Front Mol Neurosci, 2012 5: p. 95. [PubMed: 23060746]
20. Kissler JL, et al., The one-two punch of alcoholism: role of central amygdala dynorphins/kappa-opioid receptors. Biol Psychiatry, 2014 75(10): p. 774–82. [PubMed: 23611261]
21. Walker BM and Koob GF, Pharmacological evidence for a motivational role of kappa-opioid systems in ethanol dependence. Neuropsychopharmacology, 2008 33(3): p. 643–52. [PubMed: 17473837]

22. Berger AL, et al., Affective cue-induced escalation of alcohol self-administration and increased 22-kHz ultrasonic vocalizations during alcohol withdrawal: role of kappa-opioid receptors. Neuropsychopharmacology, 2013 38(4): p. 647–54. [PubMed: 23212453]
23. Valdez GR and Harshberger E, kappa opioid regulation of anxiety-like behavior during acute ethanol withdrawal. Pharmacol Biochem Behav, 2012 102(1): p. 44–7. [PubMed: 22487769]
24. Vijay A, et al., PET imaging reveals lower kappa opioid receptor availability in alcoholics but no effect of age. Neuropsychopharmacology, 2018 43(13): p. 2539–2547. [PubMed: 30188515]
25. Arvidsson U, et al., The kappa-opioid receptor is primarily postsynaptic: combined immunohistochemical localization of the receptor and endogenous opioids. Proc Natl Acad Sci U S A, 1995 92(11): p. 5062–6. [PubMed: 7539141]
26. Ilango A, et al., Similar roles of substantia nigra and ventral tegmental dopamine neurons in reward and aversion. J Neurosci, 2014 34(3): p. 817–22. [PubMed: 24431440]
27. Rossi MA, et al., Operant self-stimulation of dopamine neurons in the substantia nigra. PLoS One, 2013 8(6): p. e65799. [PubMed: 23755282]
28. Chen G, Kozell LB, and Buck KJ, Substantia nigra pars reticulata is crucially involved in barbiturate and ethanol withdrawal in mice. Behav Brain Res, 2011 218(1): p. 152–7. [PubMed: 20974184]
29. Crowley NA, et al., Dynorphin Controls the Gain of an Amygdalar Anxiety Circuit. Cell Rep, 2016 14(12): p. 2774–83. [PubMed: 26997280]
30. Krashes MJ, et al., An excitatory paraventricular nucleus to AgRP neuron circuit that drives hunger. Nature, 2014 507(7491): p. 238–42. [PubMed: 24487620]
31. Vong L, et al., Leptin action on GABAergic neurons prevents obesity and reduces inhibitory tone to POMC neurons. Neuron, 2011 71(1): p. 142–54. [PubMed: 21745644]
32. Mazzone CM, et al., Acute engagement of Gq-mediated signaling in the bed nucleus of the stria terminalis induces anxiety-like behavior. Mol Psychiatry, 2018 23(1): p. 143–153. [PubMed: 27956747]
33. Li C, et al., Alcohol effects on synaptic transmission in periaqueductal gray dopamine neurons. Alcohol, 2013 47(4): p. 279–87. [PubMed: 23597415]
34. Li C, et al., Mu Opioid Receptor Modulation of Dopamine Neurons in the Periaqueductal Gray/Dorsal Raphe: A Role in Regulation of Pain. Neuropsychopharmacology, 2016 41(8): p. 2122–32. [PubMed: 26792442]
35. Pati D, Pina MM, and Kash TL, Ethanol-induced conditioned place preference and aversion differentially alter plasticity in the bed nucleus of stria terminalis. Neuropsychopharmacology, 2019.
36. Pleil KE, et al., Effects of chronic ethanol exposure on neuronal function in the prefrontal cortex and extended amygdala. Neuropharmacology, 2015 99: p. 735–49. [PubMed: 26188147]
37. Ford CP, Beckstead MJ, and Williams JT, Kappa opioid inhibition of somatodendritic dopamine inhibitory postsynaptic currents. J Neurophysiol, 2007 97(1): p. 883–91. [PubMed: 17122312]
38. Vardy E, et al., A New DREADD Facilitates the Multiplexed Chemogenetic Interrogation of Behavior. Neuron, 2015 86(4): p. 936–946. [PubMed: 25937170]
39. Reep RL and Winans SS, Efferent connections of dorsal and ventral agranular insular cortex in the hamster, Mesocricetus auratus. Neuroscience, 1982 7(11): p. 2609–35. [PubMed: 7155344]
40. Watabe-Uchida M, et al., Whole-brain mapping of direct inputs to midbrain dopamine neurons. Neuron, 2012 74(5): p. 858–73. [PubMed: 22681690]
41. Nair-Roberts RG, et al., Stereological estimates of dopaminergic, GABAergic and glutamatergic neurons in the ventral tegmental area, substantia nigra and retrorubral field in the rat. Neuroscience, 2008 152(4): p. 1024–31. [PubMed: 18355970]
42. Gonzalez-Hernandez T and Rodriguez M, Compartmental organization and chemical profile of dopaminergic and GABAergic neurons in the substantia nigra of the rat. J Comp Neurol, 2000 421(1): p. 107–35. [PubMed: 10813775]
43. Liu XB and Jones EG, Localization of alpha type II calcium calmodulin-dependent protein kinase at glutamatergic but not gamma-aminobutyric acid (GABAergic) synapses *in thalamus and cerebral cortex*. Proc Natl Acad Sci U S A, 1996 93(14): p. 7332–6. [PubMed: 8692993]

44. Sik A, et al., The absence of a major Ca2+ signaling pathway in GABAergic neurons of the hippocampus. Proc Natl Acad Sci U S A, 1998 95(6): p. 3245–50. [PubMed: 9501248]
45. Beul SF and Hilgetag CC, Towards a “canonical” agranular cortical microcircuit. Front Neuroanat, 2014 8: p. 165. [PubMed: 25642171]
46. Tremblay R, Lee S, and Rudy B, GABAergic Interneurons in the Neocortex: From Cellular Properties to Circuits. Neuron, 2016 91(2): p. 260–92. [PubMed: 27477017]
47. Naka A and Adesnik H, Inhibitory Circuits in Cortical Layer 5. Front Neural Circuits, 2016 10: p. 35. [PubMed: 27199675]
48. German DC and Manaye KF, Midbrain dopaminergic neurons (nuclei A8, A9, and A10): three-dimensional reconstruction in the rat. J Comp Neurol, 1993 331(3): p. 297–309. [PubMed: 8514911]
49. Celada P, Paladini CA, and Tepper JM, GABAergic control of rat substantia nigra dopaminergic neurons: role of globus pallidus and substantia nigra pars reticulata. Neuroscience, 1999 89(3): p. 813–25. [PubMed: 10199615]
50. Tepper JM and Lee CR, GABAergic control of substantia nigra dopaminergic neurons. Prog Brain Res, 2007 160: p. 189–208. [PubMed: 17499115]
51. Vijay A, et al., PET imaging reveals sex differences in kappa opioid receptor availability in humans, in vivo. Am J Nucl Med Mol Imaging, 2016 6(4): p. 205–14. [PubMed: 27648372]
52. Wang YJ, et al., Sex difference in kappa-opioid receptor (KOPR)-mediated behaviors, brain region KOPR level and KOPR-mediated guanosine 5’-O-(3-[35S]thiotriphosphate) binding *in the guinea pig*. J Pharmacol Exp Ther, 2011 339(2): p. 438–50. [PubMed: 21841040]
53. Altemus M, Sarvaiya N, and Neill Epperson C, Sex differences in anxiety and depression clinical perspectives. Front Neuroendocrinol, 2014 35(3): p. 320–30. [PubMed: 24887405]
54. Avery JA, et al., Major depressive disorder is associated with abnormal interoceptive activity and functional connectivity in the insula. Biol Psychiatry, 2014 76(3): p. 258–66. [PubMed: 24387823]

Highlights

- KOR modulates a midbrain-projecting microcircuit in layer 5 of the insular cortex
- Dynorphin reduces GABA neuron excitability in layer 5 of the insular cortex
- Dynorphin increases excitatory drive in midbrain-projecting insular cortex neurons
- KOR DREADD inhibition of insula GABA neurons recapitulates the effects of dynorphin
- Insula projections release glutamate on substantia nigra GABA and dopamine neurons

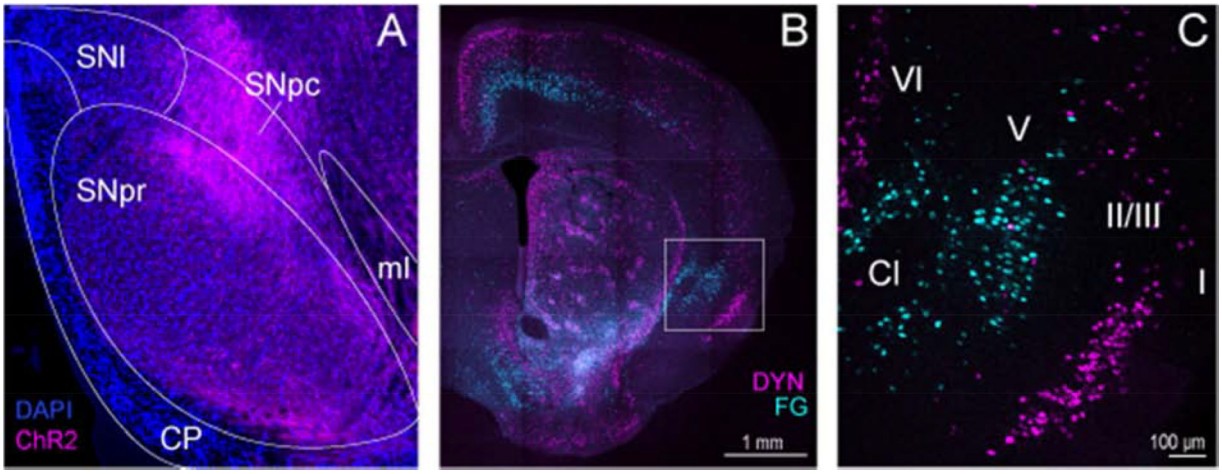

Figure 1. Circuit tracing of agranular insular cortex (IC) inputs to the substantia nigra (SN).

(A) Viral-mediated anterograde tracing via injection of AAV-CAMKII-ChR2-mCherry into the IC was used to map long-range projections to the SN. Channelrhodopsin-2 (ChR2)-positive fibers (pseudocolored magenta) from the IC were distributed throughout the GABA-enriched SN pars reticulata (SNpr) and dopamine dense SN pars compacta (SNpc). Nuclei were counterstained with DAPI (blue). (B-C) Injection of the fluorescent retrograde tracer Fluoro-Gold (FG) was used to confirm IC inputs to the SN, and FG-positive neurons (pseudocolored cyan) were distributed in layers 5 and 6 of the IC. Conversely, dynorphin (DYN) cells (pseudocolored magenta) are densely expressed in layer 2/3 of the IC, and do not overlap with layer 5 IC-SN projection neurons (pseudocolored cyan). Roman numerals indicate cortical layers; Cl, claustrum; CP, cerebral peduncle; ml, medial lemniscus; SNl, lateral substantia nigra

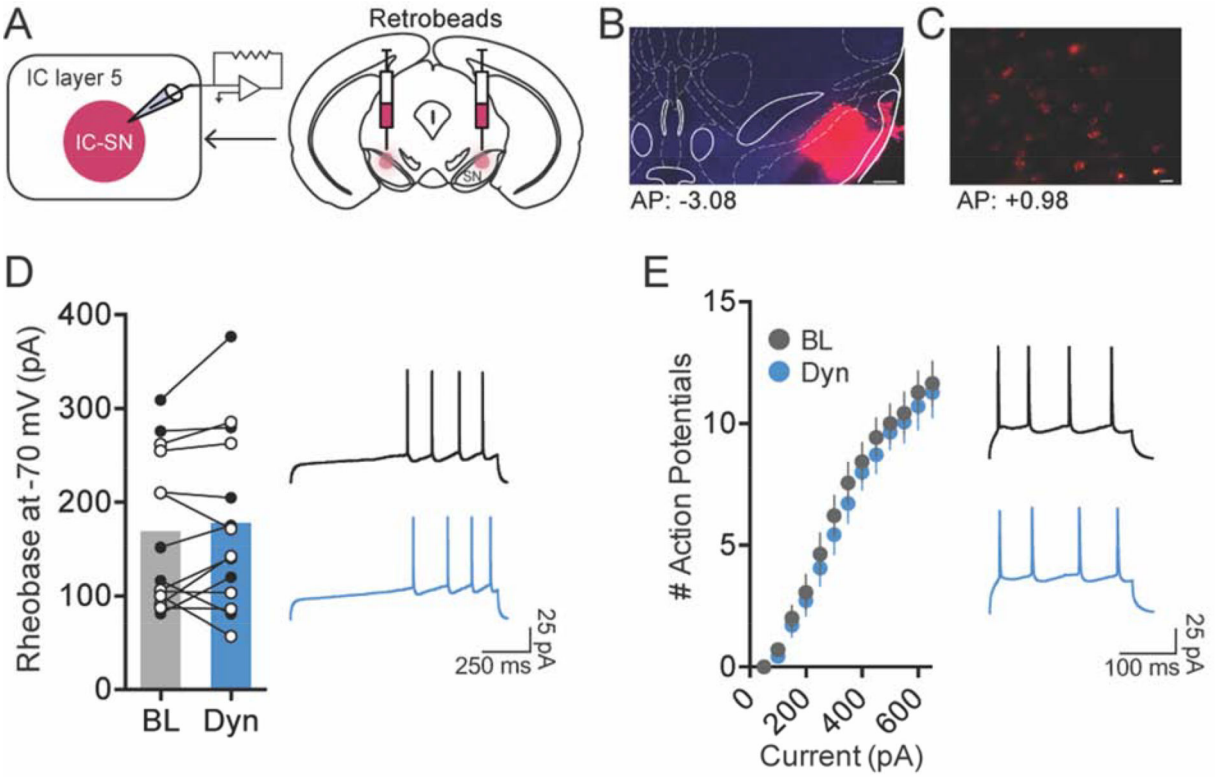

Figure 2. Activation of kappa opioid receptor (KOR) did not reduce the excitability of SN-projecting IC neurons.

(A) To label IC-SN neurons, fluorescent retrobeads were injected into the SN 7–10d before whole-cell recordings. (B) Representative images of retrobeads infused in the SN; scale bar, 250 μm and (C) retrobead labeling in IC-SN neurons; scale bar, 20 μm. Coordinates correspond to anterior-posterior (AP) position relative to bregma. (D) The minimum current required to elicit an action potential (rheobase) did not change from baseline (BL) following 10 min bath application of dynorphin A (Dyn, 300 nM); females data points are in open (white) circles, males are in closed (black) circles. (E) Dynorphin A did alter the number of action potentials fired per current injection step. Right panels in D and E show representative traces of current-injected firing in IC-SN neurons held at a common potential of −70 mV before (black) and after (blue) Dyn wash-on during a ramp protocol of 100 pA/1 s beginning at 200 pA (D) and at a 400 pA/250 ms current step (E). n = 3 mice/sex; BL, baseline; Dyn, dynorphin A

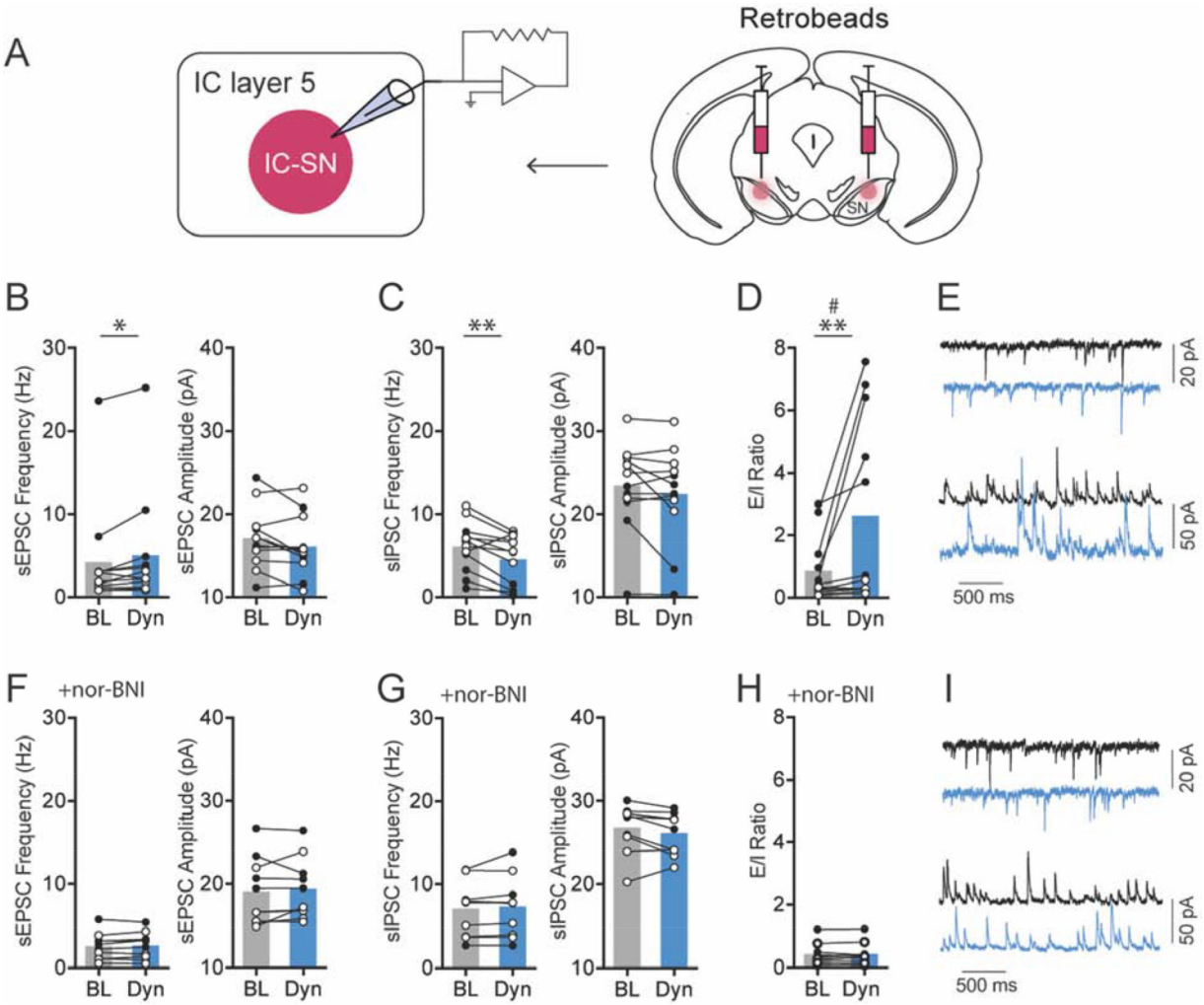

Figure 3. KOR activation increased glutamate release and reduced GABA release on SN-projecting IC neurons.

(A) IC-SN neurons were labeled for whole-cell recordings using fluorescent retrobeads injected into the SN. (B) Compared to baseline (BL), 10 min bath application of dynorphin A (Dyn, 300 nM) significantly increased spontaneous excitatory postsynaptic current (sEPSC) frequency but not amplitude, *$p < 0.05$ and (C) reduced spontaneous inhibitory postsynaptic current (sIPSC) frequency but not amplitude in IC-SN cells, **$p < 0.01$. (D) Dyn increased sEPSC/sIPSC (E/I) ratio in a sex-dependent manner; sex × drug interaction, #$p < 0.01$; significant increase in E/I in male mice, **$p < 0.01$. (E) Representative traces of sEPSCs (top) and sIPSCs (bottom) at baseline (black) and following Dyn (blue) wash-on. (F) The increase in sEPSC frequency, (G) decrease in sIPSC frequency, and (H) increase in E/I ratio by Dyn were blocked by pre-application of the KOR antagonist nor-BNI (100 nM), and sEPSC and sIPSC amplitude was not impacted. (I) Representative traces of sEPSCs and sIPSCs at baseline (black) and following Dyn (blue) wash-on in slices pretreated with nor-BNI. Females, open circles; males closed circles; n = 3 mice/sex (normal aCSF), n = 3 mice/sex (nor-BNI); BL, baseline; Dyn, dynorphin A

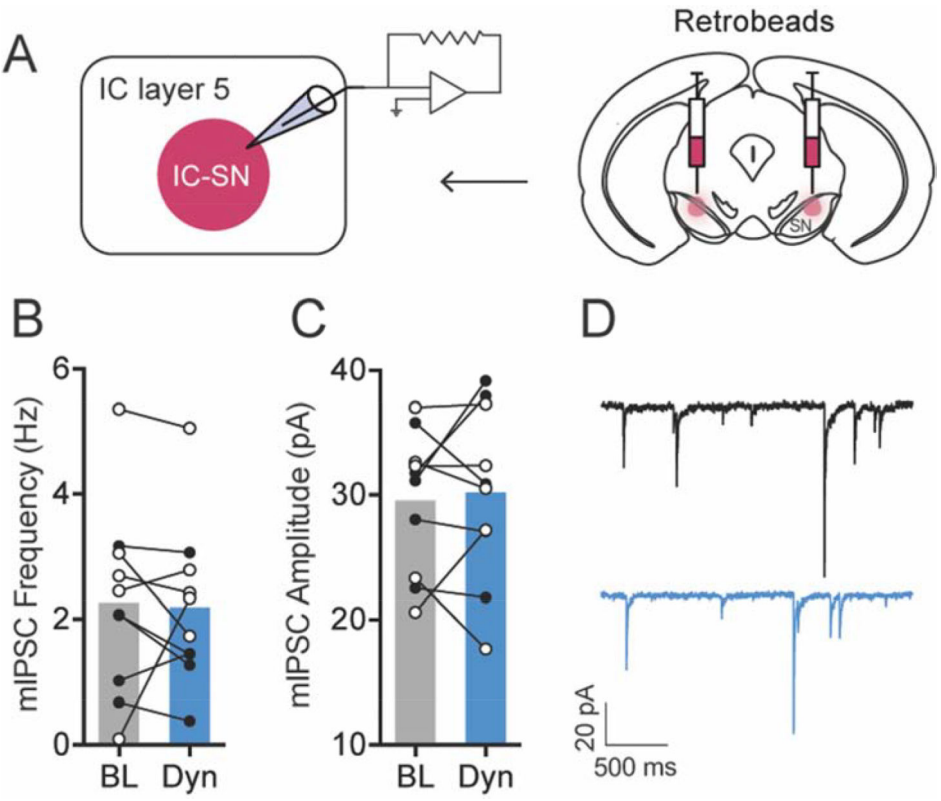

Figure 4. KOR activation had no effect on miniature inhibitory postsynaptic current (mIPSC) in SN-projecting IC neurons.

(A) Fluorescent retrobeads were used to label IC-SN neurons for whole-cell recordings. (B) Frequency and (C) amplitude of mIPSC were not significantly altered following 10 min bath application of dynorphin A (300 nM). (D) Representative traces of mIPSC from an IC-SN neuron before (black) and after (blue) Dyn wash-on. Females, open circles; males closed circles; n = 3 mice/sex; BL, baseline; Dyn, dynorphin A

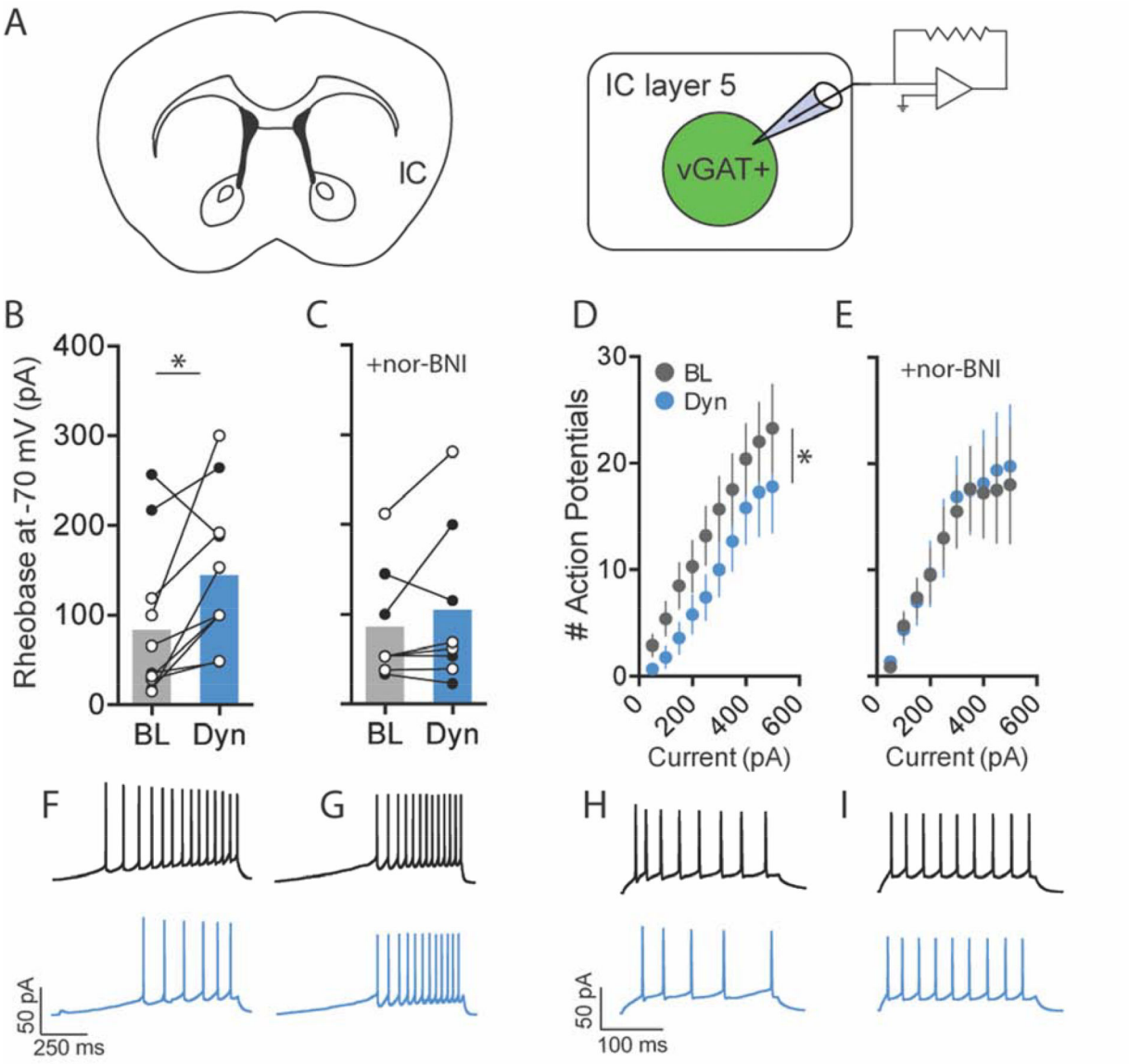

Fig. 5.

Activation of KOR reduced the excitability of GABA neurons in layer 5 of the IC. (A) For whole-cell recordings, GABA neurons in layer 5 of the IC were identified using a vGAT^{L10a} reporter strain of mouse. (B) Compared to baseline (BL), 10 min bath application of dynorphin A (Dyn, 300 nM) significantly increased the minimum current required to elicit an action potential (rheobase) in GABA neurons, (C) an effect that was blocked by pre-application of the KOR antagonist nor-BNI (100 nM); females, open circles; males closed circles. (D) Dyn decreased action potential firing to increasing current steps, (E) but not in the presence of nor-BNI. (F–I) Representative traces of current-injected firing in layer 5 GABA neurons held at a common potential of −70 mV before (black) and after (blue) Dyn wash-on (F) during a ramp protocol of 100 pA/1 s and (H) at a 100 pA/250 ms current step. (G, I) Dyn-induced reductions in current injected firing were blocked in slices treated with nor-BNI. n = 2–3 mice/sex (normal aCSF), n = 2 mice/sex (nor-BNI); *$p < 0.05$; BL, baseline; Dyn, dynorphin A.

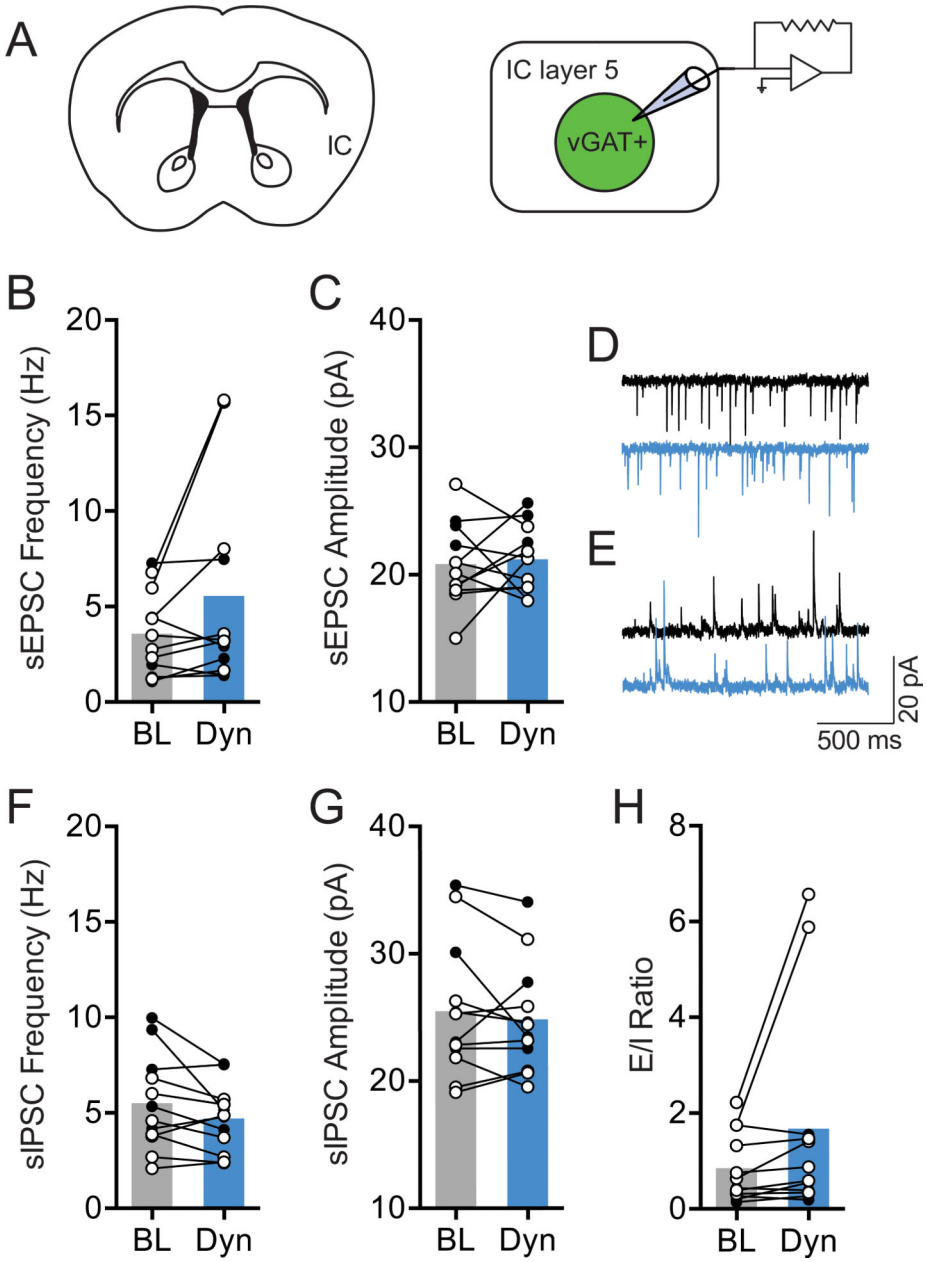

Figure 6. KOR activation did not affect synaptic transmission on GABA neurons in layer 5 of the IC.

(A) vGAT^{L10a} reporter mice were used to identify GABA neurons in layer 5 of the IC for whole-cell recording. (B) In GABA neurons, 10 min bath application of dynorphin A (Dyn, 300 nM) did not alter the frequency or (C) amplitude of spontaneous excitatory postsynaptic current (sEPSC) from baseline (BL). (D) Representative traces of sEPSCs and (E) sIPSCs at baseline (black) and following Dyn (blue) wash-on. (F) There was no effect of Dyn on spontaneous inhibitory postsynaptic current (sIPSC) frequency, (G) amplitude, or (H) sEPSC/sIPSC (E/I) ratio in layer 5 IC GABA neurons. Females, open circles; males closed circles; n = 2–3 mice/sex; BL, baseline; Dyn, dynorphin A

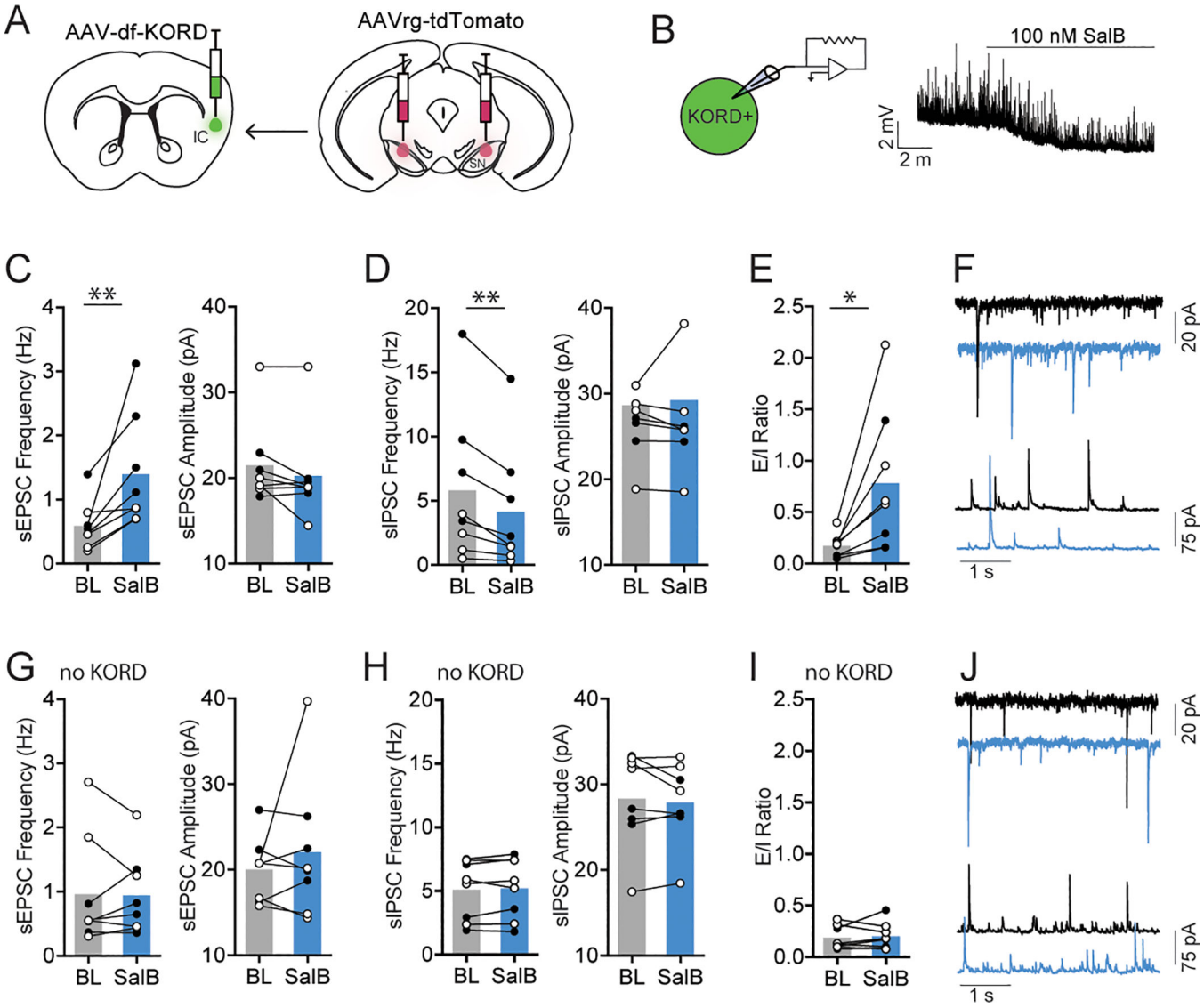

Fig. 7.

Chemogenetic inhibition of IC GABA neurons alters E/I ratio in IC-SN neurons. (A) A KOR-derived DREADD (KORD) was expressed unilaterally in the IC of vGAT-cre mice and IC-SN neurons were labeled for whole cell recordings with a retrograde AAV-tdTomato injected into the SN. (B) KORD-expressing vGAT neurons in the IC were robustly hyperpolarized by salvinorin B (SalB, 100 nM) wash-on. (C) Compared to baseline (BL), 10 min bath application of SalB significantly increased spontaneous excitatory postsynaptic current (sEPSC) frequency but not amplitude and (D) reduced spontaneous inhibitory postsynaptic current (sIPSC) frequency but not amplitude in IC-SN cells, (E) resulting in a significant increase in sEPSC/sIPSC (E/I) ratio. (F) Representative traces of sEPSCs (top) and sIPSCs (bottom) at baseline (black) and following SalB (blue) wash-on. (G-J) In non-KORD expressing tissue, SalB did not affect (G) sEPSC frequency or amplitude, (H) sIPSC frequency or amplitude, or (I) E/I ratio in IC-SN neurons. (J) Representative traces of sEPSCs and sIPSCs at baseline (black) and following SalB (blue) wash-on. Females, open

circles; males closed circles; n = 2 mice/sex; *p < 0.05, **p < 0.01; BL, baseline; SalB, salvinorin B.

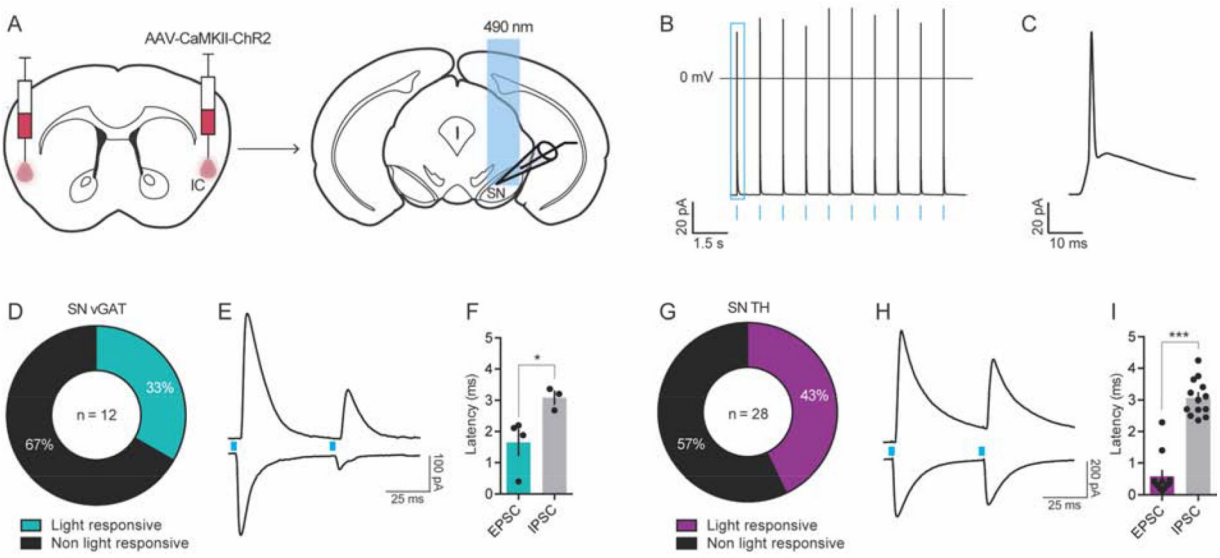

Figure 8. The IC projects polysynaptically onto GABA and dopamine neurons of the SN.

(A) Channelrhodopsin-2 (ChR2)-assisted circuit mapping was used to identify the cell populations in the SN innervated by IC inputs. (B) Functional expression of ChR2 was confirmed using patch clamp electrophysiology, which showed that IC ChR2+ neurons fired action potentials in response to optogenetic cell body stimulation (blue bars) at 1 Hz. (C) Zoomed in example of a light-evoked action potential from panel B (in blue square). (D-I) Optically-evoked excitatory (oEPSC) and inhibitory postsynaptic current (oIPSC) were recorded in SN vGAT (D-F) and TH (G-I) neurons after ChR2 stimulation. (D) 33% of vGAT neurons were light responsive, with n = 4 / 12 showing a time-locked (< 2 ms latency) oEPSC and n = 3 / 12 cells showing a delayed (> 3 ms latency) polysynaptic oIPSC to a 5 ms blue-light pulse (F). (G-I) In TH neurons, 43% were light-responsive, with n = 12 / 28 showing a time-locked (< 1 ms latency) oEPSC and n = 13 / 28 showing a delayed (> 3 ms latency) polysynaptic oIPSC (I). Representative traces of light-evoked oEPSC (bottom) and oIPSC (top) in vGAT neurons (E) and TH neurons (H) in the SN during the paired pulse stimulation protocol, where blue boxes indicated light pulse stimulus onset. Latency of oIPSC onset following light stimulation was significantly greater than that of oEPSC illustrating the polysynaptic nature of this input to SN vGAT (F) and TH neurons (I), *p < 0.05, ***p < 0.001; TH, tyrosine hydroxylase; vGAT, vesicular GABA transporter